PHYSICAL REVIEW B **71**, 174408 (2005)

Random-phase approximation for critical temperatures of collinear magnets with multiple sublattices: GdX compounds (X=Mg,Rh,Ni,Pd)

J. Rusz*
Department of Electronic Structures, Faculty of Mathematics and Physics, Charles University, Ke Karlovu 5,
121 16 Prague 2, Czech Republic
and Institute of Physics, Academy of Sciences of the Czech Republic, Cukrovarnická 10, 162 53 Prague, Czech Republic

I. Turek[†] and M. Diviš
Department of Electronic Structures, Faculty of Mathematics and Physics, Charles University, Ke Karlovu 5,
121 16 Prague 2, Czech Republic
(Received 23 December 2004; published 11 May 2005)

An efficient scheme for evaluating the critical temperatures of ferromagnetic, antiferromagnetic, and ferrimagnetic crystals with multiple sublattices is presented. The approach is based on a pairwise Heisenberg Hamiltonian and a random-phase approximation (Tyablikov's decoupling) for magnon Green's functions. The pair exchange interactions are derived from self-consistent electronic structure calculations using a magnetic force theorem. The developed technique is applied to hexagonal gadolinium and its selected intermetallic compounds GdX (X=Mg,Rh,Ni,Pd) with CsCl and CrB structures. The calculated critical temperatures are quite sensitive to a neglect of the nonmagnetic (X) element; their values are in a fair agreement with experiment.

DOI: 10.1103/PhysRevB.71.174408 PACS number(s): 75.10.Hk, 71.70.Gm, 75.10.Jm

I. INTRODUCTION

Before the era of relatively fast and cheap computers, the description of solid state was possible only within crude approximations or using model approaches. These model approaches were successful from many aspects. However, their parameters remained undetermined, or in better cases, they had to be obtained by fitting experimental data.

The Heisenberg model Hamiltonian has been introduced in the first half of last century. Since then it has often been used for evaluation of finite temperature magnetic properties of different systems. A number of approximations have been devised to its treatment. The simplest one is the mean-field approximation (MFA). It allows us to obtain critical temperatures and magnetizations very easily. However, it is known, that it overestimates the exact critical temperature given by the model.

On the opposite side, there are Monte Carlo simulations, which, if introduced properly, can lead to exact results of the Heisenberg model. Unfortunately, these methods are rather demanding from the point of view of computer resources, particularly, when there is a large number of parameters, i.e., for long-range exchange interaction, which occur in metals.

An approximative method better than MFA is based on random-phase approximation (RPA). This method employs the Green's functions technique. Its central idea is a decoupling of higher order Green's function in the equation of motion. RPA was introduced for spin $1/2$ by Tyablikov[1] and later extended and generalized by Callen[2] for Bravais lattices with general spin quantum number. While it does not describe correctly all details of low-temperature behavior, it performs much better than MFA. An important property of RPA is, that for positive exchange interactions, RPA critical temperature is lower than the exact critical temperature.[3] It means, that combining MFA with RPA provides an upper and lower bound of critical temperatures (although, one would naturally expect, that RPA result is closer to the exact result).

In recent years, interest for model hamiltonians is increasing due to the possibility to obtain values of their parameters from modern parameter-free theory of electronic structure of solids. The enormous growth of computer power allows to perform rather realistic *ab initio* bandstructure calculations at the zero temperature within density functional theory.[4] Reliable nonzero temperature *ab initio* calculational schemes[5] remain an unsolved task and quantum Monte Carlo methods[6] are still too demanding on the computer time to be practical. But we can relatively easily calculate model parameters *ab initio* and then study nonzero temperature properties within the given model. This has been demonstrated by a number of authors for finite-temperature properties of ferromagnetic transition-metal-based systems studied within the classical Heisenberg Hamiltonian.[7–13] The concept of local magnetic moments in metallic systems is justified by an adiabatic approximation[14,15] valid especially for systems with well-developed magnetic moments (Mn, Fe).

Theoretical investigations of nonzero temperature properties (specific heat, susceptibility, resistivity) of rare-earth-based systems employed the crystal-field Hamiltonian during the last decade.[16–19] Recent studies have indicated that the classical Heisenberg model can serve as a good starting point for quantitative estimations of their magnetic transition temperatures.[20,21]

In the rare-earth metals and intermetallic compounds, the exchange interactions are usually of the Ruderman-Kittel-Kasuya-Yosida (RKKY) type.[22] These interactions are long range and this leads to a vast number of non-negligible Heisenberg Hamiltonian parameters. This is a difficult task for Monte Carlo simulations and thus the RPA would be a

1098-0121/2005/71(17)/174408(9)/$23.00

very useful tool. Although in the published literature there are works describing the RPA approach to fully compensated antiferromagnets,[23,24] to our best knowledge, the RPA formalism has not yet been described in sufficient detail and generality for the case of multiple-sublattice magnetic structures containing nonequivalent sublattices.

The extension to multiple sublattice cases turned out to be nontrivial and it is the main topic of this paper, which is organized as follows. The formalism is given in the Sec. II and the method of solution of the RPA equations is described in the Sec. III. In Secs. IV and V we apply the developed formalism to selected Gd-based compounds. First, in Sec. IV we briefly describe the method we used to obtain exchange parameters and in Sec. V we use them to evaluate the critical temperature within the MFA and the extended RPA formalism. Finally, in the Appendix we give a proof for a multiple sublattice structure, that the RPA provides lower critical temperatures than the MFA.

II. FORMALISM

The isotropic Heisenberg Hamiltonian can be written in the following form:

$$\hat{H} = -\sum_{ij,AB} J_{ij}^{AB} \hat{\mathbf{s}}_{i,A} \cdot \hat{\mathbf{s}}_{j,B} - \sum_{i,A} b_A \hat{s}_{i,A}^z, \tag{1}$$

where J_{ij}^{AB} are exchange parameters; i,j are unit cell indices; A,B are sublattice (basis site) indices; b_A is proportional to the magnetic field parallel to the z axis at basis site A; and $\hat{\mathbf{s}}_{i,A} \equiv (\hat{s}_{i,A}^x, \hat{s}_{i,A}^y, \hat{s}_{i,A}^z)$ are spin operators operating in unit cell i on basis site A. S_A is then the magnitude of the spin at basis site A. The crystal periodicity is reflected in the relation $J_{ij}^{AB} = J_{i-j,0}^{AB}$; the on-site exchange parameters are zero $J_{ii}^{AA} = 0$.

The developed formalism is based on Green's function technique. We define the (retarded) Green's function (analogically to Callen[2])

$$G_{ij}^{AB}(a;\tau) = -\frac{i}{\hbar}\Theta(\tau)\langle[\hat{s}_{i,A}^+(\tau), \exp(a\hat{s}_{j,B}^z)\hat{s}_{j,B}^-]\rangle, \tag{2}$$

where a is an auxiliary parameter and $[\hat{X},\hat{Y}] = \hat{X}\hat{Y} - \hat{Y}\hat{X}$ is a commutator. Here $\hat{s}_{i,A}^{\pm} = \hat{s}_{i,A}^x \pm i\hat{s}_{i,A}^y$; their time dependence is understood within the Heisenberg picture. $\Theta(\tau)$ is a step function, i.e., $\Theta(\tau) = 1$ for $\tau \geqslant 0$, zero otherwise. The mean value in Eq. (2) means $\langle\hat{A}\rangle = \mathrm{Tr}[\rho\hat{A}] = \mathrm{Tr}[\exp(-\beta\hat{H})\hat{A}] / \mathrm{Tr}[\exp(-\beta\hat{H})]$ with $\hat{H}$ being the Heisenberg Hamiltonian, Eq. (1), and $\beta = 1/k_B T$ with k_B being the Boltzmann constant and T a temperature.

The equation of motion for the Green function leads to

$$\frac{\partial}{\partial\tau}G_{ij}^{AB}(\tau) = -\frac{i}{\hbar}\delta(\tau)\langle[\hat{s}_{i,A}^+, \exp(a\hat{s}_{j,B}^z)\hat{s}_{j,B}^-]\rangle - \frac{1}{\hbar^2}\Theta(\tau) \times \langle[[\hat{s}_{i,A}^+(\tau), \hat{H}], \exp(a\hat{s}_{j,B}^z)\hat{s}_{j,B}^-]\rangle. \tag{3}$$

The double commutator can be easily evaluated and after the RPA decoupling according to Tyablikov[1] $\langle[\hat{s}_{i,A}^+\hat{s}_{j,B}^z, \hat{X}(-\tau)]\rangle \approx \langle\hat{s}_{j,B}^z\rangle\langle[\hat{s}_{i,A}^+, \hat{X}(-\tau)]\rangle$ we get closed (but infinite) set of equations for the Green's function

$$\begin{aligned}\frac{\partial}{\partial\tau}G_{ij}^{AB}(a;\tau) = &-\frac{i}{\hbar}\delta(\tau)\langle[\hat{s}_{i,A}^+, \exp(a\hat{s}_{j,B}^z)\hat{s}_{j,B}^-]\rangle \\ &+ \frac{2i}{\hbar}\sum_{k,C} J_{ik}^{AC}[\langle\hat{s}_{i,A}^z\rangle G_{kj}^{CB}(\tau) - \langle\hat{s}_{k,C}^z\rangle G_{ij}^{AB}(\tau)] \\ &- \frac{i}{\hbar}b_A G_{ij}^{AB}(a;\tau).\end{aligned} \tag{4}$$

This infinite set of equations can be reduced to a finite set taking an advantage of the translation symmetry of the crystal. After performing Fourier transformation in time $[F(\omega) = \int(d\omega/2\pi)e^{-i\omega\tau}F(\tau)]$ and a lattice Fourier transformation $[F_{AB}(\mathbf{q}) = \Sigma_l e^{-i\mathbf{q}\cdot\mathbf{R}_l}F_{l0}^{AB}]$, our set of equations reduces to

$$\begin{aligned}(\hbar\omega - b_A)G_{AB}(a;\omega,\mathbf{q}) = &\frac{1}{2\pi}\langle[\hat{s}_A^+, \exp(a\hat{s}_B^z)\hat{s}_B^-]\rangle\delta_{AB} \\ &- 2\sum_C \{J_{AC}(\mathbf{q})\langle\hat{s}_A^z\rangle G_{CB}(a;\omega,\mathbf{q}) \\ &- J_{AC}(\mathbf{0})\langle\hat{s}_C^z\rangle G_{AB}(a;\omega,\mathbf{q})\}\end{aligned} \tag{5}$$

or in the more matrixlike form we can write

$$\begin{aligned}\sum_C \left\{\hbar\omega\delta_{AC} - \delta_{AC}\left(b_A + \sum_D 2J_{AD}(\mathbf{0})\langle\hat{s}_D^z\rangle\right) \right. \\ \left. + \langle\hat{s}_A^z\rangle 2J_{AC}(\mathbf{q})\right\} G_{CB}(\omega,\mathbf{q}) \\ = \frac{1}{2\pi}\langle[\hat{s}_A^+, \exp(a\hat{s}_B^z)\hat{s}_B^-]\rangle\delta_{AB}.\end{aligned} \tag{6}$$

For convenience, we define a matrix $\mathbb{N}(\mathbf{q})$

$$N_{AB}(\mathbf{q}) = \delta_{AB}\left(\frac{b_A}{2} + \sum_C J_{AC}(\mathbf{0})\langle\hat{s}_C^z\rangle\right) - \langle\hat{s}_A^z\rangle J_{AB}(\mathbf{q}). \tag{7}$$

With the help of this matrix we can express the Green's function in the following form:

$$G_{AB}(\omega,\mathbf{q}) = \frac{1}{2\pi}\langle[\hat{s}_A^+, \exp(a\hat{s}_B^z)\hat{s}_B^-]\rangle[\{\hbar\omega\mathbb{1} - 2\mathbb{N}(\mathbf{q})\}^{-1}]_{AB}. \tag{8}$$

The fluctuation-dissipative theorem (FDT) states that[25]

$$\langle\hat{Y}\hat{X}(\tau)\rangle = -\int d\omega e^{i\omega\tau}\frac{2\hbar\,\mathrm{Im}\,G_{\hat{X}\hat{Y}}^{(r)}(\omega)}{e^{\beta\hbar\omega} - 1}. \tag{9}$$

Application of FDT for $\hat{X} \equiv \hat{s}_A^+$ and $\hat{Y} \equiv \exp(a\hat{s}_A^z)\hat{s}_A^-$ at $\tau = 0$ leads to the linear relation between the mean value of product of operators and their commutator

$$\langle\exp(a\hat{s}_A^z)\hat{s}_A^-\hat{s}_A^+\rangle = \langle[\hat{s}_A^+, \exp(a\hat{s}_A^z)\hat{s}_A^-]\rangle\lambda_A, \tag{10}$$

where a-independent parameters λ_A can be expressed using Eqs. (7)–(9) as

$$\lambda_A = -\frac{1}{\Omega}\int d\omega \int d\mathbf{q}\frac{2\hbar\,\mathrm{Im}\{[(\hbar\omega + i0^+)\mathbb{1} - 2\mathbb{N}(\mathbf{q})]^{-1}\}_{AA}}{e^{\beta\hbar\omega} - 1}$$
$$= \frac{1}{\Omega}\int d\mathbf{q}\sum_B U_{AB}(\mathbf{q})\frac{1}{e^{2\beta\nu_B(\mathbf{q})} - 1}U^{-1}_{BA}(\mathbf{q}), \tag{11}$$

where columns of $\mathbb{U}(\mathbf{q})$ are right eigenvectors of non-Hermitean matrix $\mathbb{N}(\mathbf{q})$ and $\nu_B(\mathbf{q})$ are corresponding right eigenvalues; Ω is the volume of the first Brillouin zone (BZ).

The last equation in expression (11) holds only if all eigenvalues of $\mathbb{N}(\mathbf{q})$ are real (for all $\mathbf{q}$) and if there exists an eigenvector for each eigenvalue. These conditions coincide with the physical requirements, that poles of Green's function must be real and of first order. Violation of these conditions spoils the formalism and indicates, that the assumed collinear magnetic structure is not consistent with the exchange interactions J_{ij}^{AB} entering the calculation.

By writing $\mathbb{N}(\mathbf{q}) = \mathbb{S}\mathbb{K}(\mathbf{q})$, where $S_{AB} = \delta_{AB}\langle\hat{s}_A^z\rangle$ and $K_{AB}(\mathbf{q}) = \Sigma_C J_{AC}(\mathbf{0})(\langle\hat{s}_C^z\rangle/\langle\hat{s}_A^z\rangle) - J_{AB}(\mathbf{q})$ we can rewrite the eigenproblem (we drop the $\mathbf{q}$ dependence for a while) $\mathbb{N}\mathbf{x} = \nu\mathbf{x}$ into an equivalent generalized eigenvalue problem $\mathbb{K}\mathbf{x} = \nu\mathbb{S}^{-1}\mathbf{x}$, where matrices $\mathbb{S}$ and $\mathbb{K}$ are Hermitean ($\mathbb{S}$ is moreover diagonal). From the basic properties of the generalized eigenvalue problem we can conclude, that for ferromagnets all eigenvalues are real (because $\mathbb{S}^{-1}$ is then positive definite), while for antiferromagnets and ferrimagents this is not guaranteed. Therefore for antiferromagnets and ferrimagnets we always need to check, whether all the eigenvalues are real.

We define an auxiliary function $\Phi_A(a) \equiv \langle\exp(a\hat{s}_A^z)\rangle$. Then $\langle(\hat{s}_A^z)^n\rangle = (\partial_a)^n\Phi_A(a)|_{a=0}$. Using this function after straightforward but lengthy operator-algebra manipulations we can rewrite Eq. (10) into a differential equation for $\Phi_A(a)$[2]

$$\Phi_A''(a) + \Phi_A'(a)\frac{\lambda_A e^{-a} + (\lambda_A + 1)}{\lambda_A e^{-a} - (\lambda_A + 1)} - \Phi_A(a)S_A(S_A + 1) = 0. \tag{12}$$

It is interesting to note, that these differential equations are fully independent, but their solutions are coupled through a-independent λ_A constants, which depend on $\langle\hat{s}_A^z\rangle$ of all sublattices. This independency of resulting differential equations allowed us to use basis-site independent parameter a in the definition of Green's function (2).

Under the boundary conditions

$$\Phi_A(0) = 1, \tag{13}$$

$$\prod_{m=-S_A}^{S_A}(\partial_a - m)\Phi_A(a)|_{a=0} = 0 \tag{14}$$

this differential equation has a known unique solution[2]

$$\Phi_A(a) = \frac{\lambda_A^{2S_A+1}e^{-aS_A} - (1 + \lambda_A)^{2S_A+1}e^{(S_A+1)a}}{[\lambda_A^{2S_A+1} - (1 + \lambda_A)^{2S_A+1}][(1 + \lambda_A)e^a - \lambda_A]}. \tag{15}$$

Its derivative at $a = 0$ gives

$$\Phi_A'(a)|_{a=0} = \langle\hat{s}_A^z\rangle$$
$$= \frac{(S_A - \lambda_A)(1 + \lambda_A)^{2S_A+1} + (S_A + 1 + \lambda_A)\lambda_A^{2S_A+1}}{(1 + \lambda_A)^{2S_A+1} - \lambda_A^{2S_A+1}}. \tag{16}$$

When we are interested in the critical temperature, these formulas can be simplified. At first, the external magnetic field is zero (i.e., all $b_A \to 0$). Then, in the limit $\beta \to \beta_C$, the mean values of moments vanish $\langle\hat{s}_A^z\rangle \to 0$ and this causes λ_A to diverge. The expansion of Eq. (16) in λ_A gives

$$\langle\hat{s}_A^z\rangle = \frac{S_A(S_A + 1)}{3\lambda_A} + O(\lambda_A^{-2}). \tag{17}$$

In this limit the eigenvalues of $\mathbb{N}(\mathbf{q})$ go to zero. Then we can simplify the exponential in the definition of λ_A [Eq. (11)] to obtain

$$\lambda_A = \frac{1}{\Omega}\int d\mathbf{q}\sum_B U_{AB}(\mathbf{q})\frac{1}{e^{2\beta\nu_B(\mathbf{q})} - 1}U^{-1}_{BA}(\mathbf{q})$$
$$\to \frac{1}{2\beta}\frac{1}{\Omega}\int d\mathbf{q}[\mathbb{N}^{-1}(\mathbf{q})]_{AA}. \tag{18}$$

Combining the last two equations we obtain

$$\langle\hat{s}_A^z\rangle = \frac{2S_A(S_A + 1)\beta_C}{3}\left\{\frac{1}{\Omega}\int d\mathbf{q}[\mathbb{N}^{-1}(\mathbf{q})]_{AA}\right\}^{-1} \tag{19}$$

which in contrast to Eq. (11) does not require a diagonalization at each $\mathbf{q}$ point in the Brillouin zone.

In the classical limit, where we replace spin operators in Eq. (1) by angular momentum vectors of size one parallel to the local magnetizations[8] (their size is absorbed into the size of $\tilde{J}_{ij}^{AB}$ exchange parameters; we will denote scaled variables by tildes), we can perform a similar derivation. The semiclassical equivalent of Eq. (16) is

$$\langle\tilde{s}_A^z\rangle = \mathcal{L}(1/\lambda_A) = \mathcal{L}\left(2\beta\left\{\frac{1}{\Omega}\int d\mathbf{q}[\tilde{\mathbb{N}}^{-1}(\mathbf{q})]_{AA}\right\}^{-1}\right), \tag{20}$$

where $\mathcal{L}(x) = \coth(x) - 1/x$ is the Langevin function.

When $b_A = 0$, in the limit $\beta \to \beta_C$ (where $\langle\tilde{s}_A^z\rangle \to 0$) Eq. (20) leads to the same result as Eq. (19) with $S_A(S_A + 1)$ replaced by one. By scaling exchange parameters $\tilde{J}_{ij}^{AB} = J_{ij}^{AB}S_A S_B$ and $\hat{\tilde{\mathbf{s}}}_A = \hat{\mathbf{s}}_A/S_A$ also in the quantum case, Eq. (19) will change into

$$\langle\hat{\tilde{s}}_A^z\rangle = \frac{2(S_A + 1)\beta_C}{3S_A}\left\{\frac{1}{\Omega}\int d\mathbf{q}[\tilde{\mathbb{N}}^{-1}(\mathbf{q})]_{AA}\right\}^{-1} \tag{21}$$

and the abovementioned classical limit is obtained for $S_A \to \infty$. The advantage of this scaled form is, that it effectively allows us to treat magnetic structures containing sublattices with different spin quantum numbers S_A including the classical spins ($S_A \to \infty$).

Using Eqs. (16) and (20) we can calculate sublattice magnetizations and Eq. (21) defines the critical temperature of a multiple sublattice ferromagnet within the RPA. These three equations are the main results of this article. Moreover, it can be shown that the RPA critical temperature is lower than the

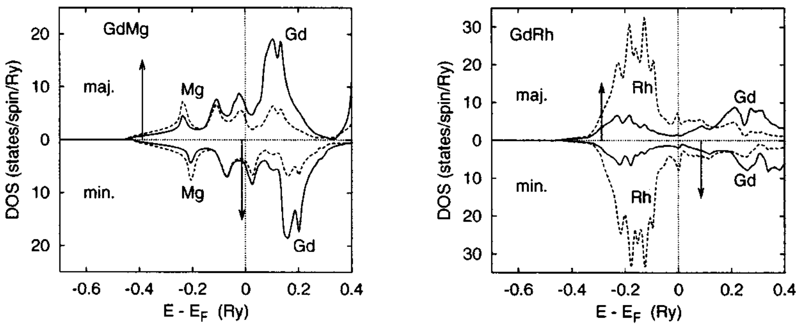

(a) GdMg (b) GdRh

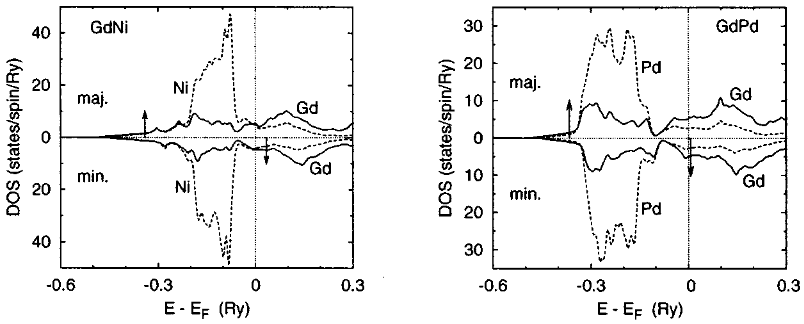

(c) GdNi (d) GdPd

FIG. 1. Site and spin-projected densities of states in GdX compounds within the open-core model. The position of arrows indicates the energy of spin-up and spin-down $4f$ states.

MFA value $T_C^{\rm RPA} < T_C^{\rm MFA}$ (see the Appendix).

Our formalism leads to identical results to the Ref. 23 for there treated magnetic orders. It can be shown, that also the spin-spiral approach in Ref. 20, which particularly for $\mathbf{Q} = (\pi/a)(1,1,1)$ leads to an antiferromagnetic order, is consistent with our results.

III. METHOD OF SOLUTION OF RPA EQUATIONS

Equations (16) together with Eqs. (11) and (7) allow us to calculate sublattice magnetizations in an iterative way. The zero-step λ_A constants can be obtained from the mean-field sublattice magnetizations[9] and then we iterate Eqs. (16) and (11) until the self-consistency is achieved.

The limiting procedure, which led to Eq. (19), has destroyed the information about absolute values of mean values of spin moments. Scaling all spins with the same constant does not change this relation. This allows us to treat all spin moments as components of vector with a fixed norm; we can set this norm to 1. These scaled moments are used to define the $\mathbb{N}(\mathbf{q})$ matrix, from which we calculate new-step moments using formula (note that β_C is omitted here)

$$\langle \hat{s}_A^z \rangle_{\rm new} = \frac{2S_A(S_A+1)}{3} \left\{ \frac{1}{\Omega} \int d\mathbf{q} [\mathbb{N}_{\rm old}(\mathbf{q})^{-1}]_{AA} \right\}^{-1}. \qquad (22)$$

If scaling the new-step moments leads within a given tolerance to the same vector as before, we have achieved the self-consistency and the scaling factor coincides with the critical temperature.

In general, there may exist more fixed points satisfying self-consistency, and correspondingly more values for critical temperature. Correctly, one should take the maximum T_C solution. However, the experience showed us, that the RPA changes only slightly the ratios between spin moments at different sites from the MFA solution, so we can easily check the physical solution by comparison with the maximum T_C MFA solution.

There is, though, a complication in the numerical implementation of BZ integration, which appears both in calculation of sublattice magnetization and critical temperatures. There occurs a divergence in the integrand for $\mathbf{q}=0$, which spoils the convergence of BZ integration. To overcome this difficulty we use an analytic deconvolution method.[15] Within this method we replace the matrix $\mathbb{N}(\mathbf{q})$ by $\mathbb{N}(\mathbf{q}) + z\mathbb{1}$ with z a small (in general complex) number. Then one can easily verify, that

$$f(0) \approx 4f(i\varepsilon) - f(2i\varepsilon) - f(\varepsilon + i\varepsilon) - f(-\varepsilon + i\varepsilon) \qquad (23)$$

up to the fourth order in ε—a small real number. The error approaches zero with decreasing ε.

IV. CALCULATION OF EXCHANGE INTERACTIONS

The exchange interactions were obtained by mapping the Heisenberg Hamiltonian to the converged *ab initio* electronic structure calculations. The same procedure was applied for example in Refs. 15 and 20, therefore we only briefly describe the method and implementation.

Electronic structure calculations were performed using tight-binding (TB) linear muffin-tin orbitals (LMTO) within the atomic spheres approximations (ASA).[26] Although this method uses an approximated (spherical) form of potential in the atomic spheres, in Gd-based compounds this should perform well, because Gd shells up to 5*s*, 5*p*, 4*f* are spherically symmetric and valence states are well represented by plane waves. Similar statements can be applied to nonmagnetic *X* sublattices in Gd*X* compounds studied in this paper. They do not carry orbital moments and their valence states strongly hybridize with Gd valence states. Still, to check TB-LMTO ASA results more thoroughly, we performed electronic structure calculations within more involved, full-potential (FP) linearized augmented plane-waves method (LAPW) implemented in the WIEN2K package.[27] Calculated densities of states and magnetic moments within both methods show a good agreement. Site and spin resolved densities of states of all four Gd*X* compounds are shown in Fig. 1.

Structure parameters were taken from experiment.[28,29] In order to improve the description of localized 4*f* states of Gd beyond standard local spin density approximation (LSDA),[4] we treated them using the open-core method.[30] For rare-earth 4*f* electrons this often performs better, than treating them within the valence band, as has been shown for example in Refs. 20 and 21.

We applied magnetic force theorem to evaluation of energy changes due to infinitesimal rotations of local moments with respect to the ordered magnetic state.[8] This procedure within TB-LMTO-ASA formalism leads to the formula

$$J_{ij}^{AB} = \frac{1}{8\pi i}\int_C \mathrm{Tr}[\Delta_{i,A}(z) g_{ij,AB}^{\uparrow}(z)\Delta_{j,B}(z) g_{ji,BA}^{\downarrow}(z)]dz. \quad (24)$$

Integration is performed along a contour in complex plane, which encircles occupied part of valence band. The trace sums over the angular momentum indices $L=(l,m)$. Quantities $g_{ij,AB}^{\sigma}(z)$ ($\sigma=\uparrow,\downarrow$—spin index) and $\Delta_{i,A}(z)$ are connected with so-called auxiliary Green functions and potential functions, respectively, of the TB-LMTO-ASA method.[26]

V. APPLICATION TO GD-BASED COMPOUNDS

A. Hexagonal close-packed Gd

Hexagonal close-packed (hcp) Gd crystal is the simplest test case for the developed formalism. It has two symmetrically equivalent Gd sublattices. This system was already studied within MFA in Ref. 21 and within RPA by Franek[31] using a simplified treatment specifically developed for hcp structure. Within this treatment the critical temperature can be calculated by an explicit formula. Our generalized treatment, which involves iterative calculation, leads for given parameters (deconvolution parameters, number of **q** points, cutoff distance) to identical results. We extend these results with an analysis of T_C dependence on cutoff distance $R_{\max}$ of exchange interactions in order to obtain the estimate of error of the calculated T_C.

The hcp Gd crystal is a metal, the exchange interactions are of long-range RKKY character. Into the calculation we included 256 symmetrically nonequivalent exchange interactions J_{ij}. This is equivalent to the $R_{\max}\approx 7.35a$, where $a=3.629$ a.u. is an experimental value of the lattice parameter (experimental value of $c/a=1.597$ was adopted).[29]

The dependence of calculated T_C on $R_{\max}$ is shown in Fig. 2. Using this figure we estimate the RPA value of the critical temperature of hcp Gd $T_C^{\mathrm{RPA}}\approx 296\ \mathrm{K}\pm 4\ \mathrm{K}$. The MFA estimate is $T_C^{\mathrm{MFA}}\approx 334\ \mathrm{K}\pm 2\ \mathrm{K}$ in agreement with published results.[21] The RPA result is in excellent agreement with the experimental value 293 K.[22]

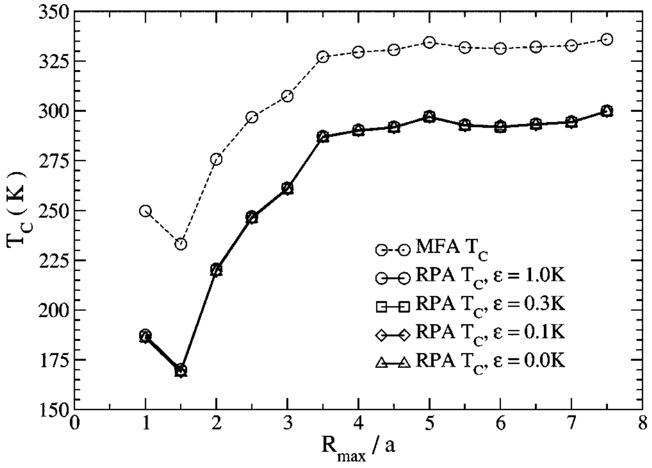

FIG. 2. Dependence of calculated T_C of hcp Gd on cutoff distance for exchange interactions within MFA (dashed curve) and RPA (solid curves; displayed for several different deconvolution parameters ε).

B. Gd*X* compounds (*X*=Rh, Mg) with CsCl structure

Intermetallic Gd*X* compounds (*X*=Mg, Rh) provide another good test cases for the developed formalism. Their structure consists of two penetrating simple cubic sublattices. Exchange interactions are of RKKY type, i.e., their magnitude decreases approximately with third power of distance, see Fig. 3. Due to their long-range character it is necessary to include J_{ij}^{AB} between rather distant neighbors. The Gd sublattice carries a large and localized magnetic moment and exchange interactions between Gd sites are the dominating mechanism for magnetic ordering. The *X* sublattice is nonmagnetic. From *ab initio* electronic structure calculations we obtain only very small induced magnetic moments for this

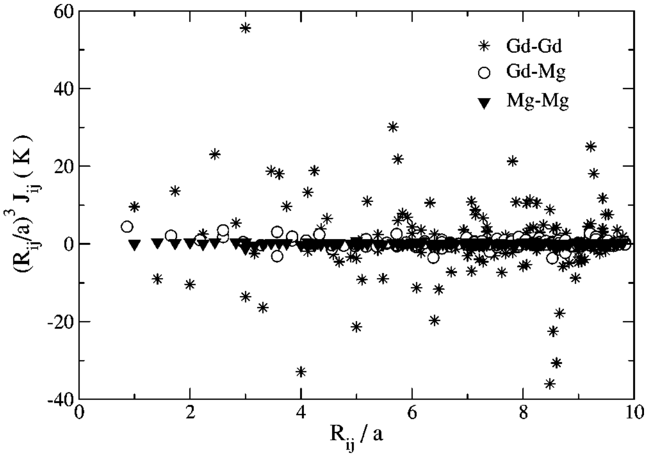

FIG. 3. Exchange interactions in GdMg between sublattices as a function of distance (in lattice parameters).

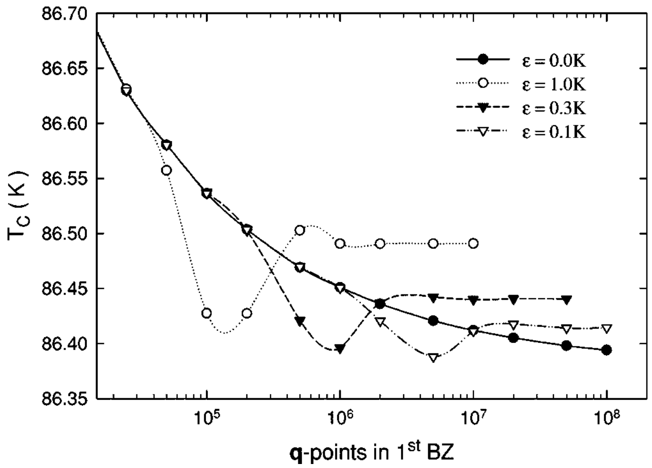

FIG. 4. Dependence of calculated critical temperature of GdMg within RPA on number of **q** points and deconvolution parameter.

sublattice. The magnitudes of exchange interactions with and within this sublattice are one or two orders smaller than Gd-Gd exchange interactions. In such cases most of the recent treatments usually completely neglect nonmagnetic sites. Applying the developed multiple sublattice RPA formalism we will show, that the influence of nonmagnetic sublattice can be in fact non-negligible and has to be included into calculations in order to obtain reliable results.

We calculated the critical temperature of two GdX (X = Mg, Rh) compounds within both MFA and RPA treatment. From the numerical point of view, within the RPA, the calculation depends on two parameters. The deconvolution parameter ε, which occurs in Eq. (23), and the number of points in the BZ sampling. The dependence of calculated critical temperature on both of these parameters is shown for GdMg in Fig. 4. We see, that the general behavior is following: the critical temperature decreases with increasing number of **q** points until reaching a narrow minimum, after which it slightly increases and stabilizes. Such behavior was observed in all treated compounds, sometimes with damped oscillations before reaching a stable value. The initial decrease can be understood in terms of decreasing influence of the divergence in the $\mathbf{q}=0$ point with growing number of **q** points. After that the calculated critical temperature stabilizes after some damped oscillations.

To test the influence of nonmagnetic sublattice on calculated critical temperatures, we did two sets of calculation. In the first one we calculated the critical temperature by including all exchange interactions for both sublattices using the developed formalism. In the second set (denoted as $\widetilde{T}_C$) we excluded all interactions with and within nonmagnetic sublattice, effectively doing a single sublattice calculation. The results are collected in the Table I. It is interesting that inclusion of nonmagnetic sublattice into the calculation leads to the increase of the calculated critical temperature (both in MFA and RPA). That increase is up to 40% (RPA for GdMg). It is important to note, that for GdRh without Rh sublattice, the RPA calculation of critical temperature did not converge. Because maximum of norm of $J_{AB}(\mathbf{q})$ matrix occurs at nonzero **q**, this indicates that in this system would occur some more complicated magnetic ordering than ferromagnetism. This however contradicts the experiment.[28] Here we just note, that for a more detailed study one can try to generalize the multiple sublattice RPA formalism in a way similar to the treatment of spin spirals in Ref. 20. Anyway, in both treated cases the influence of nonmagnetic sublattice on the results is by far not negligible.

Because of the long-range character of RKKY interaction (see Fig. 3), we were also interested in the dependence of calculated critical temperature on the cutoff distance $R_{\max}$ for included exchange parameters. The dependence of calculated critical temperature of GdMg within both RPA and MFA as a function of the cut-off distance is plotted in Fig. 5. In our calculation the maximum cutoff distance was approximately $10a$, where a is lattice parameter. This corresponds to approximately 250 symmetrically nonequivalent neighbors of a given site. The figure shows, that in these metallic systems it is very important to include interactions between rather distant neighbors. Plots of this kind are the source of error bars shown in Table I.

C. GdX compounds (X = Ni, Pd) with CrB structure

The structure of intermetallic GdX compounds with X = Ni or Pd is of CrB type. It is base centered orthorhombic structure with four sublattices (two formula units per primitive unit cell). Dominating exchange interactions are again between Gd atoms. Also in these compounds, the exchange interactions (see Fig. 6) are of RKKY type. Interestingly, we observe a faster convergence of the calculated critical temperature with respect to the $R_{\max}$ (Fig. 7) in comparison to GdX compounds with CsCl structure considered in this work.

The magnetism of the X sublattice is not yet fully clear from experimental data. In the literature there are some evidences for existence of non-negligible itinerant magnetic

TABLE I. Radii s of the TB-LMTO-ASA atomic spheres of the individual sublattices and the magnetic moments m inside them; experimental ($T_C^{\exp}$) and calculated random-phase (T_C^{RPA}) and mean-field (T_C^{MFA}) critical temperatures. The calculations, where X sublattice was neglected, are denoted by tildes.

	s_{Gd}[a.u.]	s_X[a.u.]	$m_{\mathrm{Gd}}[\mu_B]$	$m_X[\mu_B]$	$T_C^{\exp}$[K]	T_C^{RPA}[K]	$\widetilde{T}_C^{\mathrm{RPA}}$[K]	T_C^{MFA}[K]	$\widetilde{T}_C^{\mathrm{MFA}}$[K]
GdRh	3.351	3.351	7.177	−0.0842	24–29.5	21±1		33.4±0.5	16±1
GdMg	3.543	3.543	7.419	0.1645	119–120	85±1	60±1	91±1	66±1
GdNi	3.614	2.677	7.375	−0.0873	73	97.5±0.5	85.0±0.5	120.5±0.3	104.0±0.3
GdPd	3.716	2.753	7.304	−0.0321	39.5	56.5±0.5	55.0±0.5	68.3±0.1	66.2±0.1

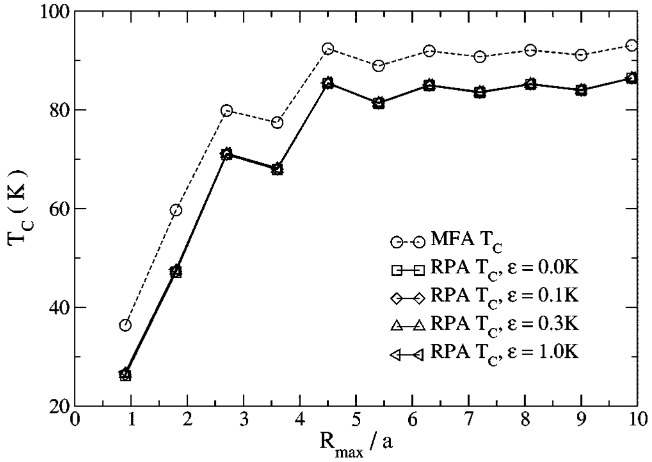

FIG. 5. Dependence of calculated critical temperature of GdMg within RPA and MFA on the cutoff distance $R_{\max}$ of included exchange parameters (a is the lattice parameter).

moments originating from Ni 3*d* states,[32,33] but this seems to be still under debate. From the calculational point of view, our DFT calculations lead to negligible magnetic moments on Ni sublattices consistently within both TB-LMTO-ASA and WIEN2K approaches, see Table I.

Again to test the importance of full four-sublattice calculation, we calculated the critical temperature also without considering the exchange interactions with and within the non-magnetic sublattice. Results are summarized in Table I. While in the GdPd the effect of nonmagnetic sublattice is at the level of 3%, in the GdNi compound including interactions with Ni sublattice seems to be very important. The calculated critical temperatures with and without Ni sublattice differ by ≈20%.

A possible explanation of this difference lies in the size of the Ni and Pd magnetic moments. Within the classical Heisenberg model the exchange parameters J_{AB} are scaled by the sizes of magnetic moments of sublattices A and B. The Pd moments (see Table I) are 2.7 times smaller than Ni moments, while Gd moments are of course comparable in both compounds. If we assume the same exchange mechanism and neglect the small differences in lattice parameters, this leads to 2.7 times smaller $J_{\mathrm{Gd-Pd}}$ exchange interactions and 7.4 times smaller $J_{\mathrm{Pd-Pd}}$ interactions in comparison to GdNi compound. (This semi-quantitatively agrees with *ab initio* calculated J_{ij}^{AB} exchange integrals.) And this is actually the order of ratio of the effects of nonmagnetic sublattices on T_C in GdNi and GdPd.

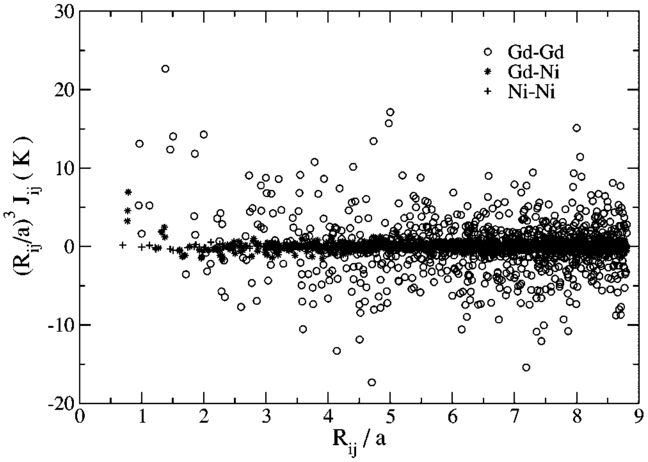

FIG. 6. Exchange interactions in GdNi between sublattices as a function of distance.

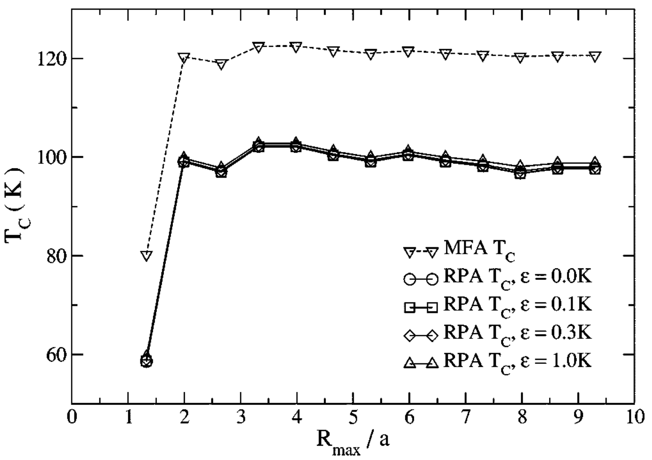

FIG. 7. Dependence of calculated critical temperature of GdNi within RPA (for several different deconvolution parameters ε) and MFA on the cutoff distance $R_{\max}$ of included exchange parameters.

In both these compounds the calculated critical temperature overestimates the experimental T_C. With nonmagnetic sublattice excluded the results are in better agreement with experiment. As we see, this is a fortuitous case and a complete treatment gives different results. Therefore we again stress, that neglecting the nonmagnetic sublattices in calculation of critical temperatures can lead to substantial errors if their effect is not verified to be really negligible.

VI. CONCLUSIONS

We extended the random phase approximation for Heisenberg Hamiltonian to allow for description of general crystal structures with multiple sublattices. This extension allowed us to calculate critical temperatures of hcp Gd and Gd*X* compounds containing more than one sublattice, where exchange interactions are of long-range (RKKY) character.

Our results have confirmed that a combination of this technique with *ab initio* calculation of exchange parameters is a promising approach to the description of nonzero temperature magnetic properties of solids. We were able to reproduce the broad scatter of the critical temperatures ranging from ~25 K for GdRh to ~300 K for hcp Gd.

As an another important result, we have shown, that the effect of nonmagnetic sublattices on magnetic properties can be non-negligible and should be considered in calculations.

ACKNOWLEDGMENTS

This work is a part of the research program MSM 0021620834 financed by the Ministry of Education of the Czech Republic. J.R. acknowledges also the support of the project AV0Z1–010–914 of the Institute of Physics, Prague.

APPENDIX: PROOF OF THE RELATION $T_C^{\mathrm{RPA}} < T_C^{\mathrm{MFA}}$

Let us transform the non-Hermitean matrix $\mathbb{N}(\mathbf{q})$ into a related Hermitean matrix $\mathbb{M}(\mathbf{q}) = \mathbb{S}^{-1/2}\mathbb{N}(\mathbf{q})\mathbb{S}^{1/2}$ with elements

$$M_{AB}(\mathbf{q}) = \delta_{AB}\left(\frac{b_A}{2} + \sum_C J_{AC}(\mathbf{0})\langle \hat{s}_C^z\rangle\right) - \sqrt{\langle \hat{s}_A^z\rangle} J_{AB}(\mathbf{q}) \sqrt{\langle \hat{s}_B^z\rangle}. \tag{A1}$$

This transformation is directly applicable only to ferromagnets due to the square roots of mean values of magnetic moments. It is evident, that both matrices have identical eigenvalues. An advantage is, that the matrix $\mathbb{V}(\mathbf{q})$ of eigenvectors of $\mathbb{M}(\mathbf{q})$ is unitary, i.e., $\mathbb{V}(\mathbf{q})\mathbb{V}^\dagger(\mathbf{q}) = \mathbb{1}$ and $\mathbb{V}^\dagger(\mathbf{q})\mathbb{M}(\mathbf{q})\mathbb{V}(\mathbf{q})$ is diagonal. It is easy to show that all Eqs. (10)–(21) remain valid, if one replaces $\mathbb{N}(\mathbf{q})$ with $\mathbb{M}(\mathbf{q})$ and $\mathbb{U}(\mathbf{q})$ with $\mathbb{V}(\mathbf{q})$, respectively. In particular, we can calculate magnetizations and critical temperatures of ferromagnets in this way. This transformation greatly simplifies the proof of the general relation between MFA and RPA critical temperatures (and also some numerics due to advantageous properties of Hermitean matrices), but its applicability to ferromagnets only is quite limiting.

Now we will show, that an antiferro- and ferrimagnets can be transformed into effective ferromagnets with the same critical temperature. Let us study the following transformation (let $\epsilon_A = \mathrm{sgn}\langle \hat{s}_A^z\rangle$):

$$\langle \hat{s}_A^z\rangle \rightarrow \epsilon_A \langle \hat{s}_A^z\rangle \text{ and } J_{ij}^{AB} \rightarrow \epsilon_A J_{ij}^{AB} \epsilon_B, \tag{A2}$$

i.e., J_{ij}^{AA} remain unchanged. An inspection of the structure of the elements of $\mathbb{N}(\mathbf{q})$ reveals that $N(\mathbf{q})_{AB} \rightarrow \epsilon_A N(\mathbf{q})_{AB}$. It is then easy to see, that for the elements of the inverted matrix we obtain $[N^{-1}(\mathbf{q})]_{AB} \rightarrow \epsilon_B [N^{-1}(\mathbf{q})]_{AB}$. Particularly, the transformed equation (19)

$$\epsilon_A \langle \hat{s}_A^z\rangle = \frac{2S_A(S_A+1)\beta_C}{3}\left\{\frac{1}{\Omega}\int d\mathbf{q}\,\epsilon_A [\mathbb{N}^{-1}(\mathbf{q})]_{AA}\right\}^{-1} \tag{A3}$$

is equivalent to original equation, but now all $\langle \hat{s}_A^z\rangle$ are positive.

This completes the proof, that transformation given by Eq. (A2) does not influence the results of calculation of critical temperatures. However, the transformed $\mathbb{N}(\mathbf{q})$ has different eigenvalues and therefore sublattice magnetizations and spin-wave spectra are different (i.e., nonphysical) after applying this transformation.

Anyway, for well defined, stable collinear magnets [no complex eigenvalues; see the discussion after Eq. (11)] we can allways calculate the critical temperatures starting from a (real or effective) ferromagnetic system [applying transformation (A2) if necessary] using the Hermitean matrix $\mathbb{M}(\mathbf{q})$ instead of $\mathbb{N}(\mathbf{q})$ in Eq. (19).

The critical temperature in the MFA is related to a (generalized) eigenvalue problem for the real symmetric matrix $J_{AB}(\mathbf{0})$, namely,

$$\sum_B J_{AB}(\mathbf{0})\langle \hat{s}_B^z\rangle = \frac{3k_B T_C^{\mathrm{MFA}}}{2S_A(S_A+1)}\langle \hat{s}_A^z\rangle. \tag{A4}$$

Note, that transformation (A2) does not influence the critical temperature either in MFA. Since the physical critical temperature corresponds to the maximum eigenvalue, we can write alternatively

$$\frac{3k_B T_C^{\mathrm{MFA}}}{2} = \max \frac{\sum_{AB} J_{AB}(\mathbf{0})\langle \hat{s}_A^z\rangle\langle \hat{s}_B^z\rangle}{\sum_A [S_A(S_A+1)]^{-1}\langle \hat{s}_A^z\rangle^2}, \tag{A5}$$

where the maximum is taken over all real values of $\{\langle \hat{s}_A^z\rangle\}$.

The RPA critical temperature is found from self-consistent conditions [cf. see Eq. (19)],

$$\langle \hat{s}_A^z\rangle^{-1} = \frac{3k_B T_C^{\mathrm{RPA}}}{2S_A(S_A+1)}\frac{1}{\Omega}\int d\mathbf{q}[\mathbb{M}^{-1}(\mathbf{q})]_{AA}, \tag{A6}$$

where the non-Hermitean matrix $\mathbb{N}(\mathbf{q})$ has been substituted (see above) by the Hermitean matrix $\mathbb{M}(\mathbf{q})$ defined by Eq. (A1) with zero external magnetic field ($b_A = 0$).

Let us consider the spectral decomposition of the matrix $\mathbb{M}(\mathbf{q})$,

$$M_{AB}(\mathbf{q}) = \sum_C V_{AC}(\mathbf{q})\mu_C(\mathbf{q})V_{CB}^\dagger(\mathbf{q}), \tag{A7}$$

where $\mathbb{V}(\mathbf{q})$ are unitary matrices diagonalizing the matrix $\mathbb{M}(\mathbf{q})$ and $\mu_C(\mathbf{q})$ are its eigenvalues. Then

$$[\mathbb{M}^{-1}(\mathbf{q})]_{AB} = \sum_C V_{AC}(\mathbf{q})\mu_C^{-1}(\mathbf{q})V_{CB}^\dagger(\mathbf{q}). \tag{A8}$$

Let us assume that the matrix $\mathbb{M}(\mathbf{q})$ (for the particular set of $\{\langle \hat{s}_A^z\rangle\}$ satisfying the RPA self-consistency condition) is positive definite almost everywhere in the BZ. This condition coincides with a stability of the studied collinear magnetic structure. With the use of the well-known inequality between the arithmetic and harmonic averages of positive quantities, one can derive a relation

$$\begin{aligned}\frac{1}{\Omega}\int d\mathbf{q}[\mathbb{M}^{-1}(\mathbf{q})]_{AA} &= \frac{1}{\Omega}\int d\mathbf{q}\sum_C V_{AC}(\mathbf{q})\mu_C^{-1}(\mathbf{q})V_{CA}^\dagger(\mathbf{q})\\ &> \left[\frac{1}{\Omega}\int d\mathbf{q}\sum_C V_{AC}(\mathbf{q})\mu_C(\mathbf{q})V_{CA}^\dagger(\mathbf{q})\right]^{-1}\\ &= \left[\frac{1}{\Omega}\int d\mathbf{q}M_{AA}(\mathbf{q})\right]^{-1}\\ &= \left[\sum_C J_{AC}(\mathbf{0})\langle \hat{s}_C^z\rangle\right]^{-1}.\end{aligned} \tag{A9}$$

In the last step we employed the sum rule

$$\frac{1}{\Omega}\int d\mathbf{q}J_{AA}(\mathbf{q}) = 0, \tag{A10}$$

that is equivalent to vanishing of the on-site exchange parameters in the real space ($J_{ii}^{AA} = 0$).

From the last inequality (A9) and the RPA-selfconsistency condition (A6) we obtain

$$\sum_B J_{AB}(\mathbf{0})\langle \hat{s}_B^z\rangle > \frac{3k_B T_C^{\mathrm{RPA}}}{2S_A(S_A+1)}\langle \hat{s}_A^z\rangle \qquad (A11)$$

which after multiplication by $\langle \hat{s}_A^z\rangle$ and summation over A yields a relation

$$\frac{3k_B T_C^{\mathrm{RPA}}}{2} < \frac{\sum_{AB} J_{AB}(\mathbf{0})\langle \hat{s}_A^z\rangle\langle \hat{s}_B^z\rangle}{\sum_A [S_A(S_A+1)]^{-1}\langle \hat{s}_A^z\rangle^2}. \qquad (A12)$$

A comparison with the expression (A5) for the T_C^{MFA} proves finally the relation $T_C^{\mathrm{RPA}} < T_C^{\mathrm{MFA}}$.

---

*Electronic address: rusz@mag.mff.cuni.cz

†Also at Institute of Physics of Materials, Academy of Sciences of the Czech Republic, Brno

[1] S. V. Tyablikov, Ukr. Mat. Zh. **11**, 287 (1959); *Methods of Quantum Theory of Magnetism* (Plenum Press, New York, 1967).

[2] H. Callen, Phys. Rev. **130**, 890 (1963).

[3] Ya. G. Sinai, *Theory of Phase Transitions: Rigorous Results* (Pergamon, Oxford, 1982).

[4] P. Hohenberg and W. Kohn, Phys. Rev. **136**, B864 (1964); W. Kohn and L. J. Sham, *ibid.* **140**, A1133 (1965).

[5] N. D. Mermin, Phys. Rev. **137**, A1441 (1965).

[6] W. M. C. Foulkes, L. Mitas, R. J. Needs, and G. Rajagopal, Rev. Mod. Phys. **73**, 33 (2001).

[7] V. P. Antropov, B. N. Harmon, and A. N. Smirnov, J. Magn. Magn. Mater. **200**, 148 (1999).

[8] A. I. Liechtenstein, M. I. Katsnelson, V. P. Antropov, and V. A. Gubanov, J. Magn. Magn. Mater. **67**, 65 (1987).

[9] E. Sasioglu, L. M. Sandratskii, and P. Bruno, Phys. Rev. B **70**, 024427 (2004).

[10] L. M. Sandratskii and P. Bruno, Phys. Rev. B **67**, 214402 (2003).

[11] L. M. Sandratskii, Phys. Rev. B **68**, 224432 (2003).

[12] L. Bergqvist, O. Eriksson, J. Kudrnovský, V. Drchal, P. Korzhavyi, and I. Turek, Phys. Rev. Lett. **93**, 137202 (2004).

[13] J. Kudrnovský, I. Turek, V. Drchal, F. Máca, P. Weinberger, and P. Bruno, Phys. Rev. B **69**, 115208 (2004).

[14] B. L. Gyorffy, A. J. Pindor, J. Staunton, G. M. Stocks, and H. Winter, J. Phys. F: Met. Phys. **15**, 1337 (1985).

[15] M. Pajda, J. Kudrnovský, I. Turek, V. Drchal, and P. Bruno, Phys. Rev. B **64**, 174402 (2001).

[16] M. Mihalik, J. Vejpravová, J. Rusz, M. Diviš, P. Svoboda, V. Sechovský, and M. Mihalik, Phys. Rev. B **70**, 134405 (2004).

[17] M. Diviš, J. Rusz, and M. Richter, Acta Phys. Pol. B **34**, 1445 (2003).

[18] M. Diviš, J. Rusz, G. Hilscher, H. Michor, P. Blaha, and K. Schwarz, Czech. J. Phys. **52**, 283 (2002).

[19] M. Diviš, J. Rusz, and M. Richter, Czech. J. Phys. **52**, 247 (2002).

[20] I. Turek, J. Kudrnovský, M. Diviš, P. Franek, G. Bihlmayer, and S. Blügel, Phys. Rev. B **68**, 224431 (2003).

[21] I. Turek, J. Kudrnovský, G. Bihlmayer, and S. Blügel, J. Phys.: Condens. Matter **15**, 2771 (2003).

[22] J. Jensen and A. R. Mackintosh, *Rare Earth Magnetism* (Clarendon, Oxford, 1991).

[23] M. E. Lines, Phys. Rev. **135**, A1336 (1964).

[24] D. A. Yablonskiy, Phys. Rev. B **44**, 4467 (1991).

[25] N. Majlis, *The Quantum Theory of Magnetism* (World Scientific, Singapore, 2001).

[26] I. Turek, V. Drchal, J. Kudrnovský, M. Šob, and P. Weinberger, *Electronic Structure of Disordered Alloys, Surfaces and Interfaces* (Kluwer, Boston, 1997).

[27] P. Blaha, K. Schwarz, G. K. H. Madsen, D. Kvasnicka, and J. Luitz, WIEN2K, Vienna University of Technology, 2001.

[28] K. H. J. Buschow, Rep. Prog. Phys. **42**, 1373 (1979).

[29] J. R. Banister, S. Legvold, and F. H. Spedding, Phys. Rev. **94**, 1140 (1954).

[30] M. Richter, J. Phys. D **31**, 1017 (1998).

[31] P. Franek, Masters thesis, Department of Electronic Structures, Charles University, Prague, 2002.

[32] R. Mallik, P. L. Paulose, E. V. Sampathkumaran, S. Patil, and V. Nagarajan, Phys. Rev. B **55**, 8369 (1997).

[33] P. L. Paulose, S. Patil, R. Mallik, E. V. Sampathkumaran, and V. Nagarajan, Physica B **223&224**, 382 (1996).